

NRL Report 8207

Differential Cross Section and Related Integrals for the Molière Potential

G. P. MUELLER

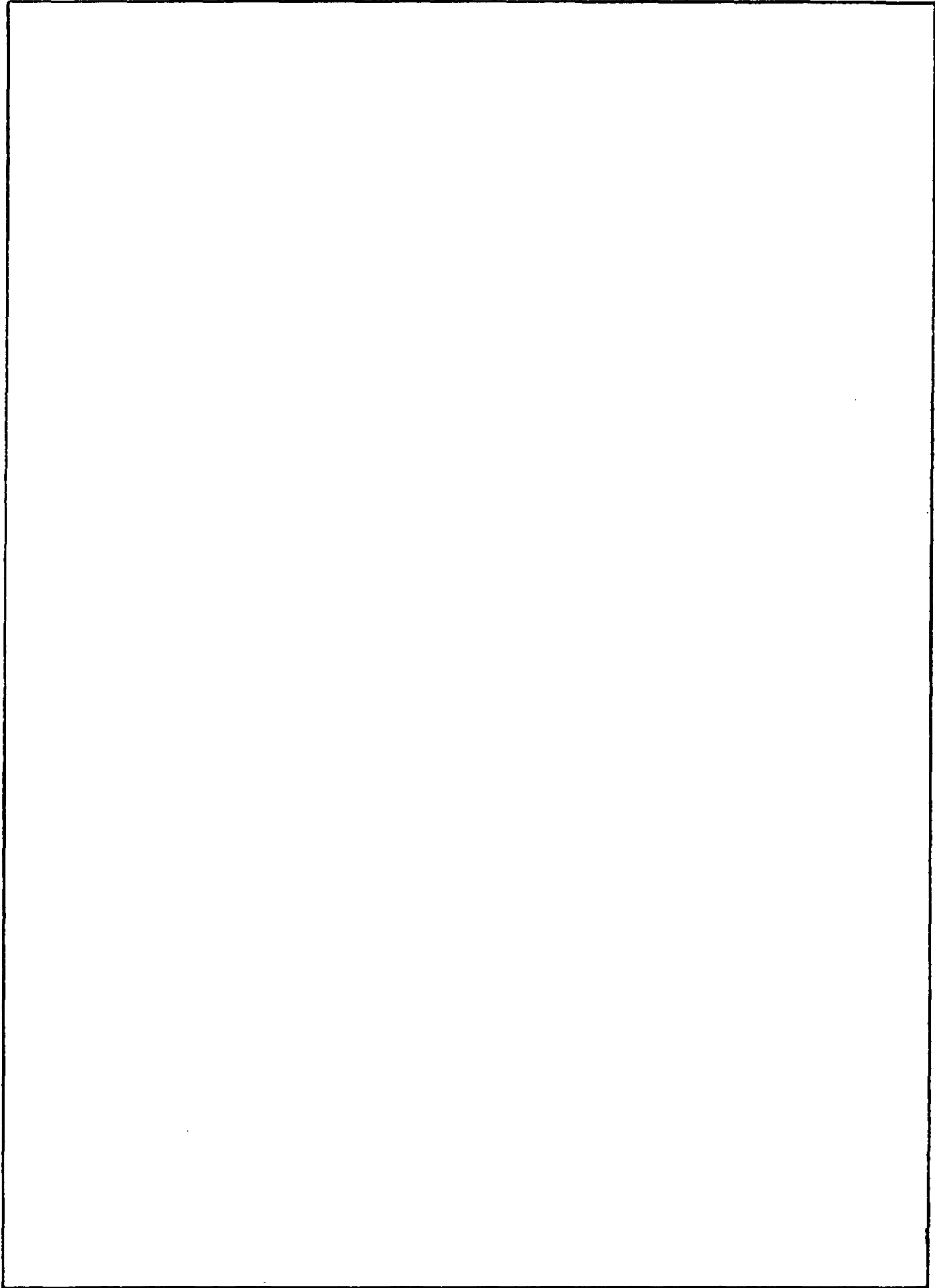
*Radiation-Matter Interactions Branch
Radiation Technology Division*

May 12, 1978



NAVAL RESEARCH LABORATORY
Washington, D.C.

SECURITY CLASSIFICATION OF THIS PAGE (When Data Entered)



SECURITY CLASSIFICATION OF THIS PAGE(When Data Entered)

CONTENTS

INTRODUCTION	1
EXACT RESULTS	4
SIMPLE FIT FOR $f_M(\eta)$	6
CONCLUSIONS	9
REFERENCES	9

DIFFERENTIAL CROSS SECTION AND RELATED INTEGRALS FOR THE MOLIÈRE POTENTIAL

INTRODUCTION

At the core of all radiation-damage and ion-range calculations for heavy-ion beams incident on bulk materials is the choice of potential that represents the interaction between the incoming ions and the lattice atoms. These potentials range from ones specifically tailored to an atom-ion pair to less accurate forms that can be used, with simply defined parameters, for any interacting pair [1]. Most of the forms in this latter category consist of some approximation to the Firsov form of the two-body Thomas-Fermi interaction.

The Thomas-Fermi potential, for an isolated atom of charge Z_2e , is usually written

$$V(r) = \frac{Z_2e}{r} \chi_T(r/a),$$

where $\chi_T(x)$ is the screening factor for the Coulomb potential and where the screening radius is

$$a = 2 \left(\frac{3\pi}{32} \right)^{2/3} \frac{\hbar^2}{me^2} Z_2^{-1/3} = 0.8853 a_0 Z_2^{-1/3}.$$

The function $\chi_T(x)$ is available in tabular form [1a]. Firsov was able to justify the adaptation of the Thomas-Fermi potential as a two-body interaction; specifically, if the quantities Z_1 and Z_2 are the atomic numbers of the incoming ion and lattice atom respectively, we write

$$V(r) = \frac{Z_1 Z_2 e^2}{r} \chi_T(r/a),$$

where we adopt the screening radius of Lindhard, Nielsen, and Scharff (LNS) [2] given by

$$a = 0.8853 a_0 Z^{-1/3},$$

$$Z = \left(Z_1^{2/3} + Z_2^{2/3} \right)^{3/2}.$$

In addition to the Thomas-Fermi screening function being available in tabular form, it has been approximated by a large variety of analytical forms. Of these forms, we are particularly interested in the Molière form [1b], given by

$$\chi_M(x) = 0.35 e^{-0.3x} + 0.55 e^{-1.2x} + 0.10 e^{-6x},$$

where $x = r/a$. The Molière screening factor falls off exponentially with large separations, whereas the Thomas-Fermi screening factor falls off as x^{-3} . It has been shown however that the Thomas-Fermi interaction falls off too slowly and that the Molière potential is a more realistic interaction for large separations [1b,3]. The Molière interaction is, for example, used by

Robinson and Torrens in their computer simulation studies of radiation damage [4]. In Fig. 1 we show the ratio of the Molière and Thomas-Fermi screening factors as a function of separation. The agreement is quite good out to the region where the exponential decay of the Molière screening factor is dominant. In this region, as we said, the Molière interaction is more realistic.

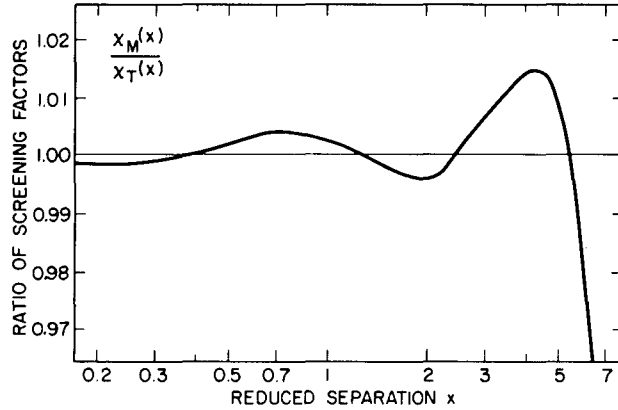


Fig. 1 — Ratio of Molière and Thomas-Fermi screening factors as a function of dimensionless separation

Although computer simulation calculations use an interaction directly, Boltzmann [5] and Lindhard [2,6] transport calculations use the scattering cross section associated with the potential. With the definitions

p = impact parameter,
 E = incident ion energy,

and

$$E_1 = \frac{A_2}{A_1 + A_2} E = \text{center of mass energy,}$$

where A_1 and A_2 are the masses in atomic units of the incoming ion and lattice atom respectively, the scattering angle is [7]

$$\theta = \pi - 2p \int_{r_{\min}}^{\infty} \frac{dr}{r^2 [1 - V(r)/E_1 - p^2/r^2]^{1/2}}, \quad (1)$$

where r_{\min} is the largest zero of the radical in the integrand. We also make use of another variable, the energy transferred in a collision,

$$T = T_m \sin^2 \theta/2,$$

where

$$T_m = \gamma E = \frac{4 A_1 A_2}{(A_1 + A_2)^2}$$

is the maximum kinetically allowed energy transfer. Corresponding to this maximum energy transfer is the minimum energy that can be carried away by the incident ion, given by

$$E_{\min} = E/\beta = \left(\frac{A_1 - A_2}{A_1 + A_2} \right)^2 E.$$

Much of the work of Lindhard and his coworkers is couched in terms of the dimensionless variables

$$\epsilon = E/E_L,$$

$$E_L = \frac{Z_1 Z_2 e^2}{a} \frac{A_1 + A_2}{A_2},$$

and

$$t = \epsilon^2 T/T_m = \epsilon^2 \sin^2 \theta/2.$$

In terms of these various definitions, the differential cross section is

$$d\sigma = -2\pi p dp = -2\pi p(t) \frac{dp(t)}{dt} dt.$$

LNS use the notation

$$d\sigma = \frac{\pi a^2}{2t^{3/2}} f(t^{1/2}) dt,$$

so that

$$f(t^{1/2}) = \frac{4}{a^2} t^{3/2} p(t) \left| \frac{dp(t)}{dt} \right|. \quad (2)$$

Out of a desire to create a simple, universal cross section, LNS now make two approximations to obtain $f(t^{1/2})$: they replace Eq. (1) by the momentum approximation [8] to the scattering angle, so that

$$\theta = -p/E_1 \int_p^\infty dr \frac{1}{r} \frac{dV(r)}{dr} (1 - p^2/r^2)^{-1/2}, \quad (3)$$

and they make the substitution

$$t = \left(\frac{\epsilon\theta}{2} \right)^2 \approx \epsilon^2 \sin^2 \theta/2.$$

By combining these approximations, we find that we can write

$$t^{1/2} = -\frac{1}{2} (p/a) \int_{p/a}^\infty dx x^{-1} \left[1 - \frac{(p/a)^2}{x^2} \right]^{-1/2} \frac{d}{dx} \left[\frac{1}{x} \chi(x) \right]. \quad (4)$$

Equation (4) provides a functional relationship between the impact parameter and the reduced energy transfer that can be used to solve Eq. (2) for $f(t^{1/2})$. The advantage of the LNS method is that the differential cross section depends on only one variable; in other words, the variable t in Eq. (4) would ordinarily depend on both p/a and ϵ , but in the LNS approximation it depends only on p/a .

Before we continue, one other point should be made. With any infinite range potential, the total cross section diverges as the energy transfer approaches zero. To bypass this difficulty,

we cut off the allowed energy transfer at a minimum value T_1 . The cutoff value will be of the order of 20 eV, dependent on the target material, and can be thought of as related to the minimum energy required to displace an atom from its lattice site. Collisions in which an energy of less than T_1 would be transferred to a lattice atom are not allowed. Roughly the same approach is taken in computer simulation calculations, where there is a maximum allowed impact parameter.

Given these considerations, the total (macroscopic) cross section is

$$N\sigma(E) = N \int d\sigma = N\pi a^2 \int_{\eta_0}^{\epsilon} d\eta \eta^{-2} f(\eta),$$

where N is the number density of lattice atoms and

$$\eta_0 = \left(\frac{E T_1}{\gamma E_L^2} \right)^{1/2}.$$

Following LNS, we can write

$$N S(E) = N\pi a^2 \frac{\gamma E_L^2}{E} \int_{\eta_0}^{\epsilon} d\eta f(\eta)$$

for the stopping cross section for elastic collisions and

$$N W(E) = N\pi a^2 \left(\frac{\gamma E_L^2}{E} \right)^2 \int_{\eta_0}^{\epsilon} d\eta \eta^2 f(\eta)$$

for the square fluctuation in energy loss. The quantities f , S , and W are provided by LNS in tabular form [2]. Manning has generated a more complete table [9]. Winterbon, Sigmund, and Sanders (WSS) [6] have created a more convenient fit to the LNS $f(\eta)$ in the form

$$f_W(\eta) = \lambda \eta^{1/3} \left[1 + (2\lambda \eta^{4/3})^{2/3} \right]^{-3/2}, \quad \lambda = 1.309.$$

Relatively convenient expressions can be found for $\sigma(E)$, $S(E)$, and $W(E)$ [10,11].

It is our intention in the rest of this report to find the $f(\eta)$ corresponding to the Molière potential and to develop convenient forms for f , σ , S , and W .

EXACT RESULTS

The integral that arises in Eq. (3) with the Molière potential is evaluated by Lehmann and Leibfried [8], with the result

$$\theta = \epsilon^{-1} \sum_{i=1}^3 b_i \lambda_i K_1(\lambda_i p/a),$$

where K_1 is the modified Bessel function,

$$\lambda_i = 0.3, 1.2, 6, \quad i = 1, 2, 3,$$

and

$$b_i = 0.35, 0.55, 0.10, \quad i = 1, 2, 3.$$

Consequently we have

$$\eta = t^{1/2} = \frac{1}{2} \sum_{i=1}^3 b_i \lambda_i K_1(\lambda_i p/a). \quad (5)$$

In terms of the variable η , Eq. (2) becomes

$$f_M(\eta) = 2 \eta^2 p/a \left| \frac{d\eta}{dp/a} \right|^{-1}, \quad (6)$$

and we find

$$\frac{d\eta}{dp/a} = -\frac{1}{2} \sum_{i=1}^3 b_i \lambda_i^2 \left[\frac{K_1(\lambda_i p/a)}{\lambda_i p/a} + K_0(\lambda_i p/a) \right]. \quad (7)$$

By using Eqs. (5), (6), and (7), we can form a table expressing the relationships between $f(\eta)$, η and p/a .

For convenience let us make the definitions

$$N \sigma_M(E) = N \pi a^2 \left[\mathcal{C}_M(\eta_0) - \mathcal{C}_M(\epsilon) \right], \quad (8)$$

$$\mathcal{C}_M(x) = \int_x^\infty d\eta \eta^{-2} f_M(\eta),$$

$$N S_M(E) = N \pi a^2 \frac{\gamma E_L^2}{E} \left[\mathcal{S}_M(\epsilon) - \mathcal{S}_M(\eta_0) \right], \quad (9)$$

$$\mathcal{S}_M(x) = \int_0^x d\eta f_M(\eta),$$

$$N W_M(E) = N \pi a^2 \left(\frac{\gamma E_L^2}{E} \right)^2 \left[\mathcal{W}_M(\epsilon) - \mathcal{W}_M(\eta_0) \right], \quad (10)$$

and

$$\mathcal{W}_M(x) = \int_0^x d\eta \eta^2 f_M(\eta).$$

The first function is trivial to evaluate, so that

$$\mathcal{C}_M(\eta) = \left[p(\eta)/a \right]^2.$$

The second quantity is

$$\mathcal{S}_M(x) = \frac{1}{2} \int_{p(x)/a}^\infty dq q \left(\sum_{i=1}^3 b_i \lambda_i K_1(\lambda_i q) \right)^2.$$

This integral can be evaluated exactly [12], yielding

$$\begin{aligned} \mathcal{S}_M(x) = & \frac{1}{4} \sum_{i=1}^3 b_i^2 s_i^2 \left[K_0^2(s_i) + \frac{2}{s_i} K_0(s_i) K_1(s_i) - K_1^2(s_i) \right] \\ & - \frac{1}{2} \sum_{\substack{i,j=1 \\ i \neq j}}^3 \frac{\lambda_i \lambda_j b_i b_j}{\lambda_i^2 - \lambda_j^2} \left[s_j K_0(s_j) K_1(s_i) - s_i K_0(s_i) K_1(s_j) \right], \end{aligned}$$

where $s_{i,j} = \lambda_{i,j} p/a$. The quantity $\mathcal{W}_M(x)$ apparently cannot be evaluated in closed form.

Figure 1 indicates the deviations of the Molière potential from the Thomas-Fermi potential. Specifically we note the series of wiggles in the ratio. These are no doubt due to the fitting of the Molière form to the Thomas-Fermi potential; they have no physical significance. In Fig. 2 we reproduce that curve, with the addition of a plot of the ratio of the Molière and Thomas-Fermi cross sections, drawn as a function of p/a . We see that the wiggles in the Molière potential, relative to the Thomas-Fermi potential, are reproduced, and indeed magnified, in the corresponding cross sections. In part this magnification is probably due to the use of the momentum approximation to calculate the scattering angle. Figure 3 provides plots of the Molière and Thomas-Fermi $f(\eta)$ functions; also shown is the WSS fit to the Thomas-Fermi $f(\eta)$ function.

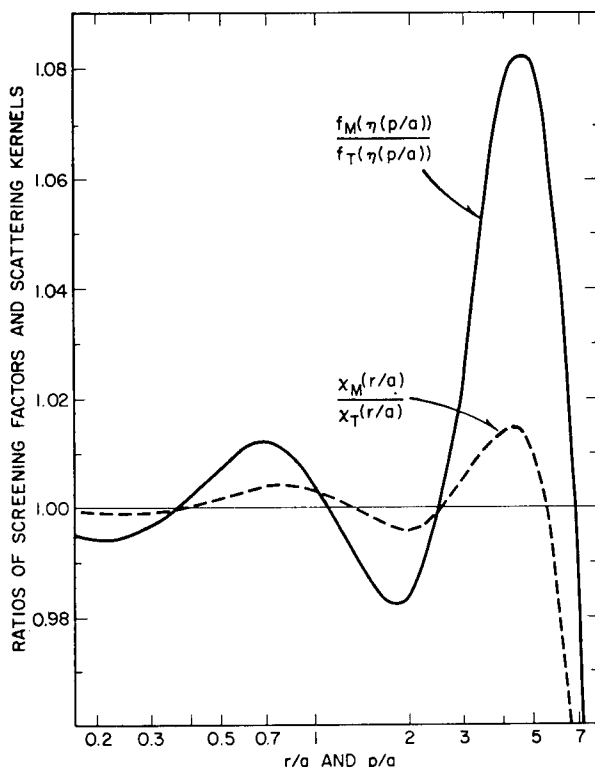


Fig. 2 — Ratio of the Molière and Thomas-Fermi screening functions as a function of r/a , and ratio of their $f(i^{1/2})$ functions, as a function of p/a

SIMPLE FIT FOR $f_M(\eta)$

It is time consuming to evaluate the exact expression (Eqs. (5), (6), and (7)) for $f_M(\eta)$; in actual use it is convenient to have some simple form to represent the cross section. We have found that

$$f(\eta) = f_1(\eta) = \alpha_0 \eta \ln \eta + \alpha_1 \eta + \alpha_2 \eta^2 + \alpha_3 \eta^3, \eta < \eta^* = 0.06,$$

$$= f_2(\eta) = \frac{\beta_1 + \eta/2}{\beta_2 + \beta_3 \eta + \eta^2}, \eta > \eta^*,$$

fits the exact $f_M(\eta)$ to better than 6% for all values of η . The values of the parameters in these equations are

$$\alpha_i = -20.45, -71, 422.097, -1429.70, \quad i = 0, 1, 2, 3,$$

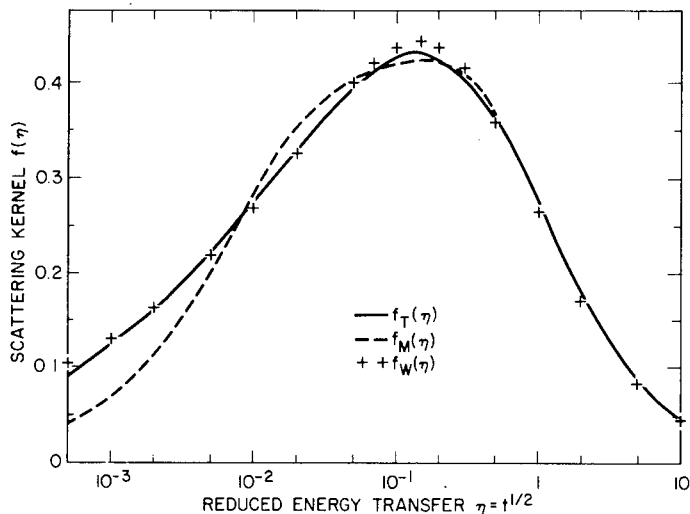


Fig. 3 — Comparison of the Molière, Thomas-Fermi, and WSS scattering functions

and

$$\beta_i = 0.007, 0.0387, 0.826), \quad i = 1, 2, 3.$$

In particular, α_2 and α_3 were chosen so that the fits in the two regions had equal values and derivatives at $\eta = \eta^*$.

The various integrals of $f(\eta)$, Eqs. (8), (9), and (10), can be evaluated in closed form. For $\eta < \eta^*$ we have

$$\mathcal{C}_1(\eta) = 148.298 - \left(\frac{1}{2} \alpha_0 \ln^2 \eta + \alpha_1 \ln \eta + \alpha_2 \eta + \frac{1}{2} \alpha_3 \eta^2 \right),$$

$$\mathcal{S}_1(\eta) = \frac{1}{2} \alpha_0 \eta^2 \left(\ln \eta - \frac{1}{2} \right) + \frac{1}{2} \alpha_1 \eta^2 + \frac{1}{3} \alpha_2 \eta^3 + \frac{1}{4} \alpha_3 \eta^4,$$

and

$$\mathcal{D}_1(\eta) = \frac{1}{4} \eta^4 \alpha_0 \left(\ln \eta - \frac{1}{4} \right) + \frac{1}{4} \alpha_1 \eta^4 + \frac{1}{5} \alpha_2 \eta^5 + \frac{1}{6} \alpha_3 \eta^6,$$

and for $\eta > \eta^*$ we have

$$\mathcal{C}_2(\eta) = \left\{ \left[(\beta_2 \beta_3 - 2\beta_1(\beta_3^2 - 2\beta_2)) P_2(\eta) + 4\beta_1 \beta_2 / \eta \right. \right. \\ \left. \left. + (\beta_2 - 2\beta_1 \beta_3) [P_1(\eta) - 2 \ln \eta] \right] / (4\beta_2^2), \right.$$

$$\mathcal{S}_2(\eta) = 0.059298 + \frac{1}{4} \left[(4\beta_1 - \beta_3) P_2(\eta) + P_1(\eta) \right],$$

and

$$\begin{aligned} \mathbb{U}_2(\eta) = & 0.079916 + \frac{1}{4} \left\{ \eta^2 + (4\beta_1 - 2\beta_3)\eta + (\beta_3^2 - \beta_2 - 2\beta_1\beta_3)P_1(\eta) \right. \\ & \left. + \left[(2\beta_1(\beta_3^2 - 2\beta_2) - \beta_3(\beta_3^2 - 3\beta_2)) \right] P_2(\eta) \right\}, \end{aligned}$$

where we write

$$\begin{aligned} P_0 &= (\beta_3^2 - 4\beta_2)^{1/2}, \\ P_1(\eta) &= \ln(\beta_2 + \eta\beta_3 + \eta^2), \end{aligned}$$

and

$$P_2(\eta) = P_0^{-1} \ln \left[(\beta_3 + 2\eta - P_0) / (\beta_3 + 2\eta + P_0) \right].$$

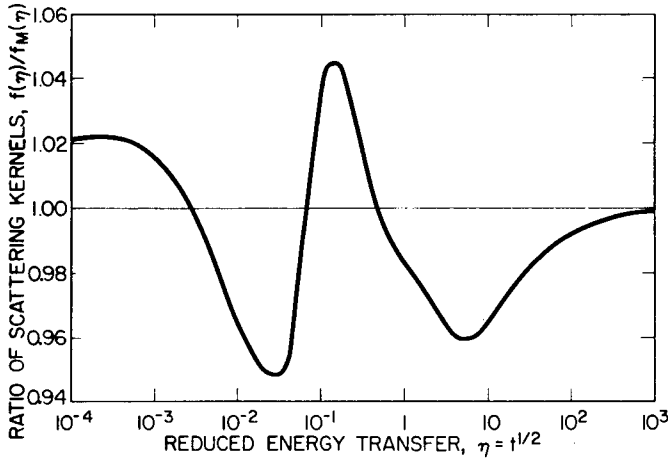


Fig. 4 — Comparison of present work with exact Molière results: ratio of scattering kernels as a function of reduced energy transfer

Figure 4 presents a comparison of our fit (f_1 and f_2) with the exact expression $f_M(\eta)$. We see that the error in $f(\eta)$ is never more than 6%. Consequently the errors in \mathcal{C} , \mathcal{S} , and \mathbb{U} will be less than 6%. Because we are now prescribing an $f(\eta)$, we are interested in what screening factor corresponds to this new $f(\eta)$. Within the spirit of the LNS approximations, embodied in Eq. (4), we can write [1c, 13, 14]

$$\begin{aligned} \chi(x) &= \frac{4x}{\pi} \int_x^\infty dq \left(q^2 - x^2 \right)^{-1/2} \eta(q) \\ &= \frac{4x}{\pi} \int_0^{\eta_x} d\eta \eta \frac{dq(\eta)}{d\eta} \left[q^2(\eta) - x^2 \right]^{-1/2}, \end{aligned}$$

where x and η_x are related by

$$x^2 = \int_{\eta_x}^\infty d\eta \eta^{-2} f(\eta).$$

In Fig. 5 we compare as a function of x the $\chi(x)$ obtained in this manner from our new $f(\eta)$ with the exact form $\chi_M(x)$. We see that $\chi(x)$ differs from $\chi_M(x)$ by less than 6%. We also show the error in $f(\eta)$ again, this time as a function of $q = p(\eta)/a$.

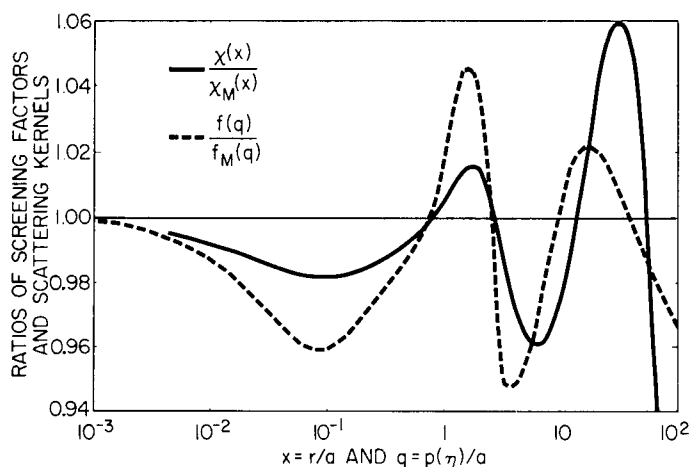


Fig. 5 — Comparison of present work with exact Molière results: ratios of scattering kernels and screening functions

CONCLUSIONS

We have created a simple differential cross section that reproduces the cross section derived from the Molière potential by the LNS method. The expressions for this $f(\eta)$ and the related integrals for total cross section, stopping power, and fluctuation in energy loss involve only simple powers and logarithms. We suggest the use of this version of the Molière cross section as a universal cross section, to replace the LNS and WSS forms.

REFERENCES

1. I.M. Torrens, *Interatomic Potentials*, Academic Press, New York, 1972: (a) Appendix 1, (b) pp. 70-73, (c) p.166.
2. J. Lindhard, V. Nielsen, and M. Scharff, Kgl. Dan. Vidensk. Selsk., Mat.-Fys. Medd. **36**, No. 10 (1968).
3. M.T. Robinson, Phys. Rev. **179**, 327 (1969).
4. M.T. Robinson and I.M. Torrens, Phys. Rev. **B9**, 5008 (1974).
5. I. Manning and D.W. Padgett, "Transport Theory of Penetration by Heavy Ions," NRL Memorandum Report 2631, Aug. 1973.
6. K.B. Winterbon, P. Sigmund, and J.B. Sanders, Kgl. Dan. Vidensk. Selsk., Mat.-Fys. Medd. **37**, No. 14 (1970).
7. H. Goldstein, *Classical Mechanics*, Addison-Wesley, Cambridge, Mass., 1950, p. 58.
8. C. Lehmann and G. Leibfried, Z. fur Phys. **172**, 465 (1963).
9. I. Manning, private communication.
10. G.P. Mueller, Radiation Effects **21**, 253 (1974).
11. K.B. Winterbon, AECL-3194, Nov. 1968.
12. A. Erdelyi, editor, *Higher Transcendental Functions*, Vol. 2, McGraw-Hill, New York, 1953, p. 90.
13. F.T. Smith, R.P. Marchi, and K.G. Dedrick, Phys. Rev. **150**, 79 (1966).
14. F. Malaguti and E. Verondini, Radiation Effects **29**, 121 (1975).